A Tactile Sensor using Three-Dimensional Structure

Hiroyuki SHINODA, Masahiro UEHARA and Shigeru ANDO
Engineering Research Institute
Faculty of Engineering, University of Tokyo
2-11-16 Yayoi, Bunkyo-ku, Tokyo 113, Japan

Abstract

In this paper, we propose a new tactile sensor for artificial fingertips utilizing a 3-D structured elastic body combined with vertical sampling pressure probes as a built-in feature extraction unit. Besides the vertical sampling principle, the presented sensor is given two new features in 1) orthogonally arranged vertical sampling probes, and 2) variable contact realized by a flexible spherical surface. Using these architecture we propose three algorithms for the sensation of 1) surface texture 2) 2-D rubbing velocity, and 3) deepness of contact. The architecture and the algorithms are examined by several experiments using scale-up model of the sensor.

1 Introduction

In this decade, various types of tactile sensors have been proposed and developed for the advanced robotics applications. The most sophisticated ones will be the 2-D arrayed pressure sensor or some position sensitive devices utilizing conductive rubber, piezoelectric effects, capacitive techniques, magnetic transduction, optical methods, and so on[1]. Recently the importance of 1) smart sensing, i.e., integrated information processing capability to provide some sophisticated tactile features to the central processing unit[2], 2) active sensing, i.e., combined sensing under a proper control of manipulators[3], 3) sensor fusion, i.e., cooperative sensing with different devices such as a TV camera[4], have been more and more recognized. This means a future design of tactile devices must depend upon what kind of tactile information is essential under the scenario of active sensing and multiple sensor fusion.

Here let us consider the human skin perceiving very fine profile or roughness of a surface texture while touching and sliding. Two most important features which we can not find in usual tactile sensors will be that the receptors are locating 3-D scatteredly and very sparsely (maximum density is only about 1 ending per mm^2 near fingertips[5]) in the elastic body of skin. This structure will suggest firstly the importance of flexibility; i.e., it enables the sensory units to maintain sufficient contact although they are moved along the complex surface. Secondly, it suggests a certain role of 3-D structure in the tactile sensation. Since the sensation of this information in 2-D arrayed static sensors requires densely located elements and sophisticated signal processing, the roles of skin mechanism have been aimed at by many recent research works. A compliant stress rate sensor[6] which detects fine surface features under sliding motion, an analysis of contact-induced stress distribution in the skin [7, 8], and its use to an inversion of the elastic contact[8], etc. But we consider there would be some additional schemes which will benefit the sophisticated tactile sensation of human.

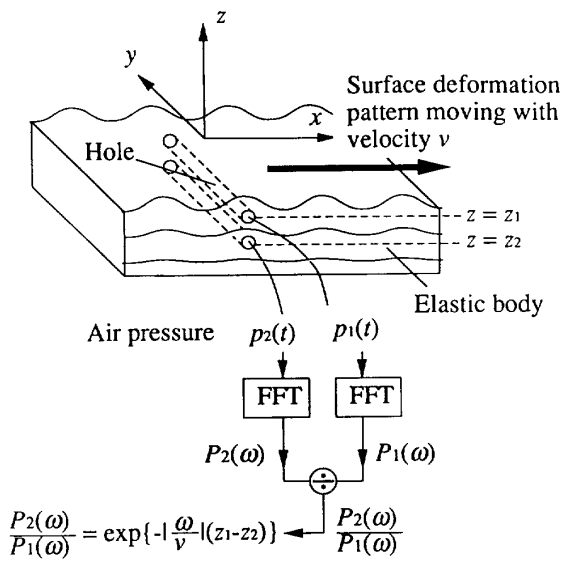

Figure 1: The divergence transfer function and vertical sampling.

The purpose of this paper is to clarify a role of 3-D flexible structure in the tactile sensation and then realize a fingertip-like tactile sensor based on this mechanism under slip motion. In section 2, we introduce

1050-4729/93 $3.00 © 1993 IEEE

the 3-D vertical sampling method for tactile sensation, and show this structure enables us to obtain 1) fine spatial frequency information of the surface texture and 2) slipping velocity between the sensor and the object[9] while holding sufficient contact with various objects. In other words, the skin is modeled as an information processing field to extract both statistic and dynamic features of a touching surface. In section 3 we extend this basic principle to a more practicable theory of fingertip tactile sensors involving an architecture of the active sensing algorithms. Two important features of our sensor reside in 1) orthogonally arranged vertical sampling probes, and 2) variable contact with a spherical surface, which are introduced to carry out some delicate and ingenuous work as is seen in the human one. Using this architecture, we propose three algorithms for the sensation of 1) surface texture, 2) 2-D rubbing velocity, and 3) deepness of contact. The architecture and the algorithms are examined by several experiments using a scale-up model of the sensor.

2 What is a Vertical Sampling Method ?

Consider for simplicity a half-infinite 2-D $x-z(z<0)$ space filled with elastic body. Consider a divergence $u \equiv \mathrm{div}\mathbf{u}$ of a displacement vector $\mathbf{u}$ caused by a touch. The divergence is easily measured as a hole pressure(see 3), and is also equivalent to a diagonal sum of a stress tensor, because

$$u = \frac{(1-2\sigma)(1+\sigma)}{E}(\sigma_{xx}+\sigma_{zz}) \tag{1}$$

where σ is a Poisson's ratio, and σ_{xx}, σ_{zz} are the diagonal stress tensor elements. Then a divergence $u(x,z)$ inside the elastic body caused by a divergence $u_0(x)$ just below the surface is shown[9] to be

$$u(x,z) = \int U_0(k)\exp(ikx+|k|z)dk \tag{2}$$

which means that spatial frequency k components of surface profile decrease, during downward propagation, in such ways that each decreasing rate is just equal to each spatial frequency k. Based on this relation and a sensor architecture shown in Fig.1, we have shown two important tactile information can be obtained by using only a couple of vertically located probes as follows[9].

2.1 Sensation of a single dominant frequency

Let $p_1(t), p_2(t)$ be temporal output signals of pressure probes which are located at $(0,z_1),(0,z_2)$ respectively. Suppose a periodic object is touched but we do not know its dominant spatial frequency k_0. Then, taking the ratio of a lower probe output $p_2(t)$ to an upper one $p_1(t)$, we know

$$\frac{p_2(t)}{p_1(t)} = \exp\{-|k_0|(z_1-z_2)\} \tag{3}$$

which means the ratio is solely determined by the spatial frequency k_0 and the probe separation z_1-z_2. Since we know the separation, the unknown spatial frequency k_0 is solved from the ratio as

$$k_0 = \frac{1}{z_1-z_2}\log\frac{p_1(t)}{p_2(t)} \tag{4}$$

2.2 Sensation of slipping velocity and surface spectra

Suppose an unknown arbitrarily textured object is slipping with a constant but unknown velocity v. Suppose temporal spectra $P_1(\omega)$ and $P_2(\omega)$ are computed from the output signals $p_1(t), p_2(t)$ respectively, and then the ratio are taken between them frequency by frequency. Notice, under the motion, a temporal frequency ω is a contribution of a spatial frequency ω/v. Therefore, by using the similar arguments as the previous section, the ratios are expressed as a unique function of the spatial frequency $|\omega/v|$ as

$$\frac{P_2(\omega)}{P_1(\omega)} = \exp\{-|\frac{\omega}{v}|(z_1-z_2)\}. \tag{5}$$

This means we can determine the velocity v of the slipping object such that

$$|v| = -\frac{|\omega|(z_1-z_2)}{\log(P_2(\omega)/P_1(\omega))}. \tag{6}$$

It will be clear, if the velocity v is determined, the surface spectra are obtained by only a simple conversion $k=\omega/v$ of the temporal spectra $P_1(\omega)$.

To understand this principle graphically, please see Fig.5. Plotting $\log|P_2(\omega)/P_1(\omega)|$ with respect to ω will result in a linear distribution. The slipping speed $|v|$ is determined by the slope of this line.

It should be emphasized that this operation is completely aliasing free, moreover because this operation is carried out by ideally continuous and homogeneous media, the execution is most reliable without complex fabrication.

3 New Architectures for Fingertip Tactile Sensors

In this section, we extend the principles described above to realize more practical tactile sensors like an artificial fingertip. In order to do this, we introduce two new architecture into the sensor as shown in Fig.2.

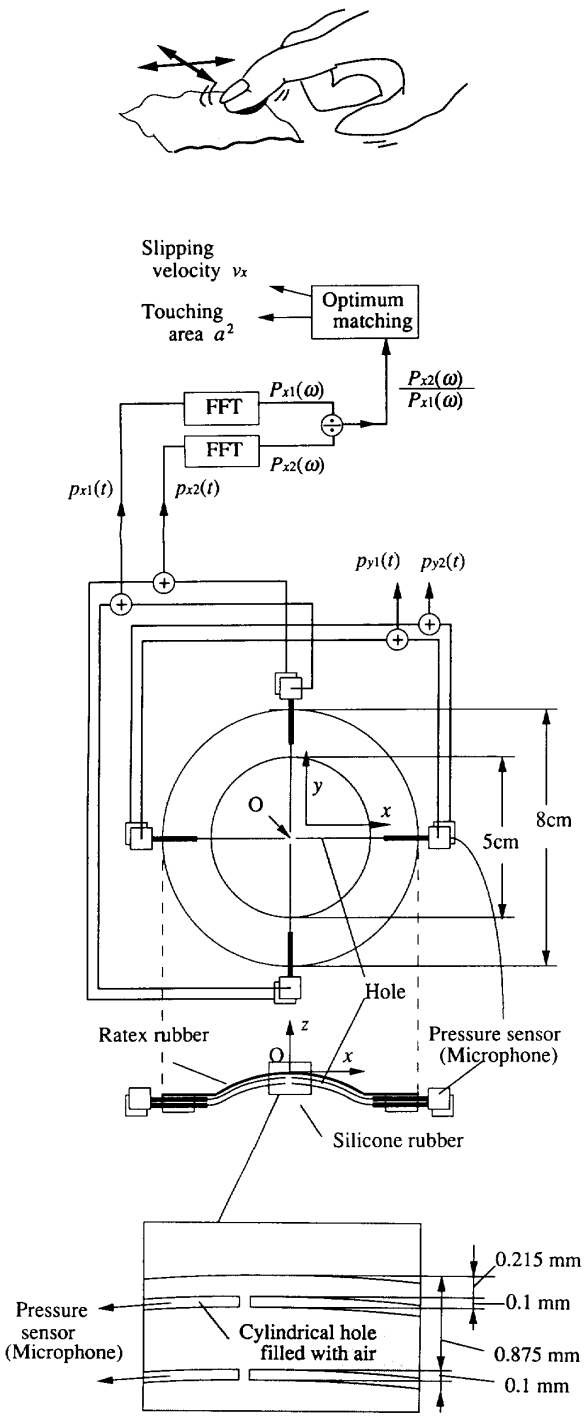

Figure 2: Spherical surface and orthogonal arrangement of vertical sampling probes.

3.1 Orthogonal 1-D probes: generation of directional sensitivity

First, we assume four 1-D probes (fine straight holes of which pressures are guided to each microphones) are locating along lines $x = 0, z = z_i$ and $y = 0, z = z_i$ $(i = 1, 2)$ in an elastic body. Since a probe pressure is an integral e.g.

$$p_{x1} = \int u(0, y, z_1) dy \ , \tag{7}$$

it can be sensitive only to variances being perpendicular to the line. In this case, a temporal output of each probe to a moving surface deformation $u_0(x - v_x t, y - v_y t)$ are expressed as

$$p_{xi}(t) = \int U_0(k_x, 0) e^{-ik_x v_x t} e^{|k_x| z_i} dk_x \tag{8}$$

$$p_{yi}(t) = \int U_0(0, k_y) e^{-ik_y v_y t} e^{|k_y| z_i} dk_y \tag{9}$$

which show we can actually pick out two orthogonal cross-sections $U_0(k_x, 0)$ and $U_0(0, k_y)$ of the 2-D spectrum $U(k_x, k_y)$ independently through the temporal spectra of each probe outputs

$$P_{xi}(\omega) = U_0(-\omega/v_x, 0) e^{|\omega/v_x| z_i} \tag{10}$$

$$P_{yi}(\omega) = U_0(0, -\omega/v_y) e^{|\omega/v_y| z_i} \tag{11}$$

3.2 Flexible convex surface: Realization of active variable contact

Secondly, we assume the sensor surface is spherically convex. The spherical surface enables us to keep good contact with various objects, but moreover it brings us an important merit for tactile sensation. Suppose a rough but globally plane object is touching at the origin of the sensor. Since the sensor is farther more flexible than the object, the sensor surface becomes flat under the contact and a normal pressure distribution there will be written as

$$p_n(x, y) = \begin{cases} p_{n0}\sqrt{1 - \frac{x^2+y^2}{a^2}} & (x^2 + y^2 \le a^2) \\ 0 & \text{(otherwise)} \end{cases} \tag{12}$$

where a is a radius of the touching area, and p_{n0} is a pressure at the origin [10].

From now on, we approximate an effective divergence pattern just below the surface $\hat{u}_0$ is a product of an actual pattern u_0 and the spatial window $w(x, y, a)$ as

$$\hat{u}_0(x, y) = w(x, y, a) u_0(x - v_x t, y - v_y t) \tag{13}$$

which is equivalent to say that its spectrum is a convolution of an original spectrum by a spectrum

$W(k_x, k_y, a)$ of $w(x, y, a)$ as

$$\hat{U}_0(k_x, k_y) = \iint W(k_x - \alpha, k_y - \beta, a) U_0(\alpha, \beta) e^{-i(\alpha v_x t + \beta v_y t)} d\alpha d\beta. \quad (14)$$

The approximation error will be experimentally examined later, but this approximation is sufficient for rough argument in this first stage. Since we can observe this window effect by using 3-D structure, then the touching area can be estimated by an algorithm discussed in next section.

4 New Algorithms for Fingertip Tactile Sensation

In this section, we describe the sensing algorithms brought by the above mentioned architecture.

4.1 Sensation of 2-D slip motion

When the touching area is sufficiently large, the window effects described above can be ignored. In this case, we can solve v_x, v_y from Eq.(10) and (11) such that

$$|v_x| = -\frac{|\omega|(z_1 - z_2)}{\log(P_{x2}(\omega)/P_{x1}(\omega))} \quad (15)$$

$$|v_y| = -\frac{|\omega|(z_1 - z_2)}{\log(P_{y2}(\omega)/P_{y1}(\omega))} \quad (16)$$

It is equivalent to say that we can determine a 2-D velocity (v_x, v_y) except signs of each components. In order to reduce window effects, the objects must be pressed rather deeply to the sensor.

4.2 Sensation of 2-D surface textures

We assume again the touching area is sufficiently large. Because of the directional selectivity of the probes, we can obtain surface texture information as follows.

First, if $U_0(k_x, 0)$ or $U(0, k_y)$ is known to have a single dominant peak but its frequency k_{x0} or k_{y0} is unknown, they are determined by taking an amplitude ratio of the probe outputs under an arbitrary (not necessarily constant) motion as ($\epsilon \equiv z_1 - z_2$)

$$k_{x0} = -\frac{1}{\epsilon} \log \frac{p_{x2}(t)}{p_{x1}(t)}, \quad k_{y0} = -\frac{1}{\epsilon} \log \frac{p_{y2}(t)}{p_{y1}(t)} \quad (17)$$

Secondly, if the surface has an arbitrary texture and is moving with an unknown but constant velocity, its 2-D spectrum is determined on two cross-sections $U_0(k_x, 0)$ and $U_0(0, k_y)$. This is because determination of the velocities v_x, v_y is equivalent to determine the cross-sections such that

$$U_0(k_x, 0) = P_{x1}(-k_x v_x) e^{-|k_x| z_1} \quad (18)$$

$$U_0(0, k_y) = P_{y1}(-k_y v_y) e^{-|k_y| z_1} \quad (19)$$

4.3 Sensation of contact deepness

In this subsection, we show an actual touching area of the sensor surface to a flat textured surface can be estimated from outputs of probes under a known motion. In following discussion, we assume the slipping direction, i.e. x-axis, is known, and the slipping velocity v_x is known. Such information is often obtained by the movement instruction given to the arm. Suppose the Fourier transform of $p_{xi}(t) = \int \hat{U}_0(k_x, k_y = 0, t) \exp(|k_x| z_i) dk_x$ combined with Eq.(14) is written by

$$P_{xi}(\omega) = \iint W(k_x + \frac{\omega}{v_x}, -\beta, a) U_0(-\frac{\omega}{v_x}, \beta) e^{|k_x| z_i} d\beta dk_x \quad (20)$$

Eq.(20) implies if we assume that the window function is separable, i.e.,

$$W(k_x, k_y, a) = W_x(k_x, a) W_y(k_y, a), \quad (21)$$

then, since P_{xi} is decomposed into

$$P_{xi}(\omega) = \int U_0(-\frac{\omega}{v_x}, \beta) W_y(-\beta, a) d\beta \int W_x(k_x + \frac{\omega}{v_x}, a) e^{|k_x| z_i} dk_x, \quad (22)$$

we can express simply the ratio of P_{x1} and P_{x2} as

$$\frac{P_{x2}(\omega)}{P_{x1}(\omega)} = \frac{\int W_x(k_x + \frac{\omega}{v_x}, a) e^{|k_x| z_2} dk_x}{\int W_x(k_x + \frac{\omega}{v_x}, a) e^{|k_x| z_1} dk_x} \equiv R(\frac{\omega}{v_x}, z_1, z_2, a). \quad (23)$$

The integrals in a numerator and a denominator of the above equation are convolutions of $\exp(|k_x| z_2)$ and $\exp(|k_x| z_1)$ respectively by $W_x(k_x)$. Because the ratio is expected to be a varying function of z_1, z_2 and a, if z_1, z_2 and v_x are known, the radius of touching area a can be determined so that the plot of $P_{x2}(\omega)/P_{x1}(\omega)$ with respect to ω fits to the ω vs. $R(\omega, v_x, z_1, z_2, a)$ curve.

Since the object is assumed to be flat, to determine the radius a is equivalent to determine the deepness of contact between sensor and object.

For calculating the function R, we use an approximation such that

$$w(x, y, a) = w_0 \exp\{-\frac{3}{2a^2}(x^2 + y^2)\} \quad (24)$$

Then $W_x(k_x, a)$ is given as

$$W_x(k_x, a) = W_0 \exp(-\frac{a^2 k_x^2}{6}). \quad (25)$$

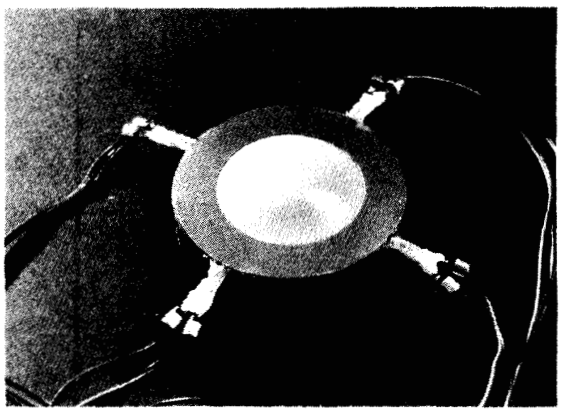

Figure 3: Photograph of the sensor.

From this approximation and Eq.(23), a curve of R is determined numerically. Therefore the radius a can be estimated through a least squares fitting so that the $\omega - \log R$ curve is closest to the plot of $\omega - \log|P_2(\omega)/P_1(\omega)|$. To help understanding, we show an very rough approximation of Eq.(23)

$$R(\frac{\omega}{v}, z_0, z_1, a) \simeq \exp\{-|\frac{\omega}{v}|(z_1 - z_2)\} \exp(\frac{3(z_1^2 - z_0^2)}{2a^2}) \tag{26}$$

From the factor $\exp(\frac{3(z_1^2-z_0^2)}{2a^2})$ in Eq.(26), we can obtain the radius a of the touching area.

5 Fabrication of Sensor

The senor body was made by molding a silicone rubber. At first it was made flatly with straight probes, and then the same material was inserted on a backing plate so that the sensor surface was lifted spherically with radius of curvature R=3cm at the top of the sensor. Each probe is a fine cylindrical hole (0.1mm diameter) in which pressure is guided to microphone. The outputs of opposite side of probes are added electrically to obtain orthogonal pairs of signals. The depth z_1, z_2 at which the probes are located are 0.265 mm and 0.925 mm respectively. Eq.(7) is good with a low frequency with which the wave length in the probe-hole air is sufficiently larger than the scale of the probe, with negligible viscosity effect.

6 Experiments

6.1 Examination of directional Selectivity

Fig.4 shows the amplitude of the output signal p_{x1} when a surface with a periodic 1-D texture is sliding

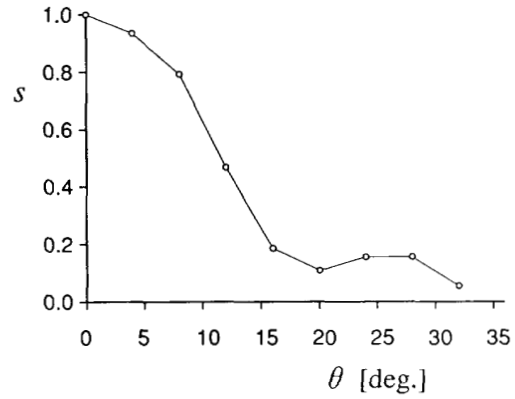

Figure 4: Selectivity of 1-D probe.

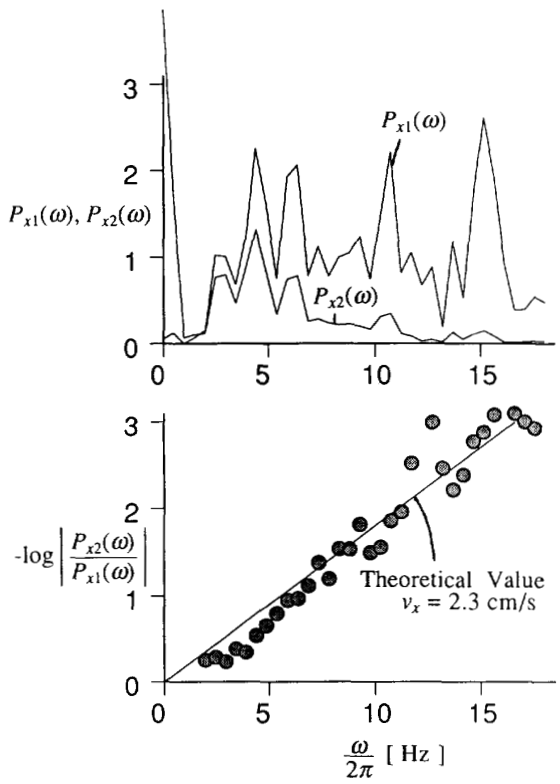

Figure 5: (a) Spectra of $p_{x1}(t)$ and $p_{x2}(t)$ when a plate of foaming polystyrene which has a random surface is slid on the sensor. (b) The ratio of P_{x2} to P_{x1}.

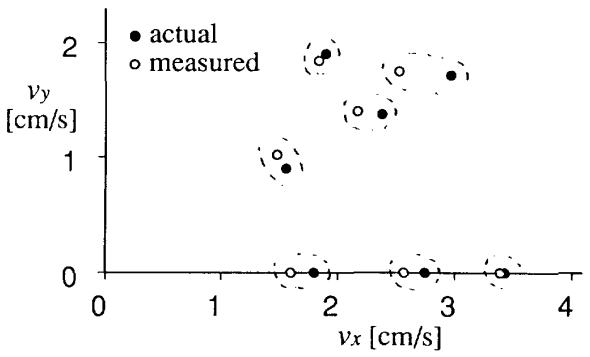

Figure 6: Sensing of 2-D slip motion for an object which has random surface (of foaming polystyrene).

on the sensor in various directions. A radius a of the touching area was 3mm. The horizontal axis indicates an angle θ between directions of the probe and the texture. The vertical axis means a selectivity s which is normalized so that $s = 1$ at $\theta = 0$. To make the periodic 1-D surface, we arranged fine long pipes with 1.5 mm pitch. This results show that directional selectivity of the 1-D probe is fairly good, therefore its output spectra can be approximated well by $U(k_x, 0)$.

6.2 Determining 2-D slip motion

Fig.5(a) shows the spectra $P_{x1}(\omega), P_{x2}(\omega)$ when a random surface made of foaming polystyrene is sliding along x-axis with a velocity v=2.3cm/s. Fig.5(b) shows the ratio $P_{x2}(\omega)/P_{x1}(\omega)$. The solid line in this figure indicates a theoretical value calculated by Eq.(15). Good agreements are found between experimental results and the theoretical values. Fig.6 shows the results of determining 2-D slip motion when the surface of foaming polystyrene is slid on the sensor with various velocities and directions. Each component of the velocity was estimated from the slope of ω - $\log|P_{i2}(\omega)/P_{i1}(\omega)|(i = x, y)$ plots as the least square solution.

6.3 Determining deepness of contact

Fig.7 shows the two way plots of $\log|P_{x2}(\omega)/P_{x1}(\omega)|$ with respect to ω obtained by rubbing an object (which is a wire net whose wire by wire intervals are 0.5mm) on the top of the sensor with contact deepness d=0.04mm and 0.16mm. The slipping speed is 4.7cm/s. The solid lines in this figure illustrate the best fitting curve of $R(\omega, a)$. The R curves fit the two kind of plots best when a=0.85mm and 2.2mm

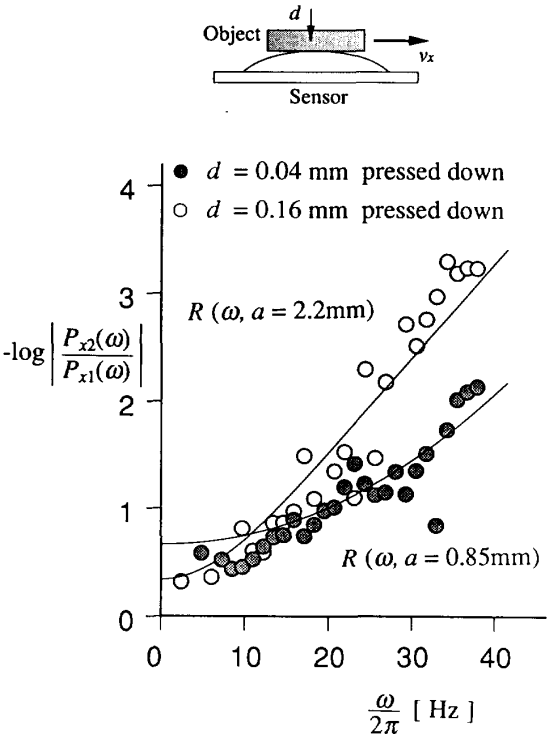

Figure 7: Plots of $\log|P_{x2}(\omega)/P_{x1}(\omega)|$ when a wire net was rubbed on the sensor with deepness of contact d= 0.04 mm and 0.16 mm. The solid curves indicate the best fitting $R(\omega, a)$ curves. The slipping velocity v_x =4.7cm/s.

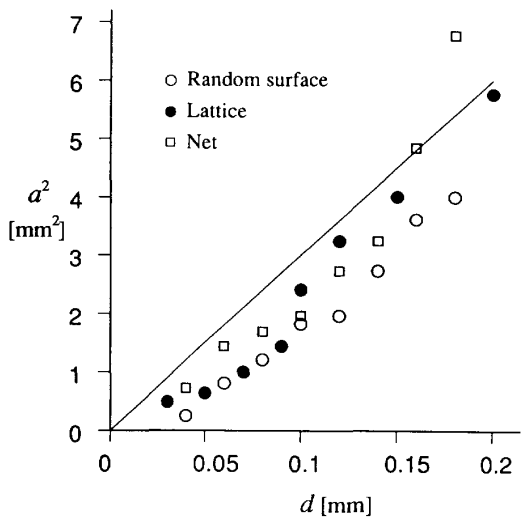

Figure 8: Sensing of touching area.

respectively. Therefore we can estimate the touching radii as 0.85mm and 2.2mm respectively. Fig.8 shows the areas a^2 estimated by this method varying the objects and the depth d at which an object was pressed down on the sensor surface. The objects are above mentioned wire net ,random surface used in subsection 6.2 and lattice used in subsection 6.1. Theoretically, the square of radius of contact area a^2 is expressed as $a^2 = Rd$ where R is a radius of curvature of sensor surface[10]. The solid line in this figure shows a calculated value when R=3cm that is the radius of curvature of the sensor. This results show the approximations adopted previous sections are reasonable, and we can believe it is sufficiently possible to estimate a contact area by using this algorithm.

7 Future Developments

Since in every experiments an actually used area of the sensor surface was within only about 5mm diameter, there will be no essential problems in down-sizing the sensor. Our goal in this respect is the size by which several sensors can be attached around a finger. Another important feature of the sensor is an active control capability of the contact deepness. To improve flexibility of the sensor, we are designing a new type of sensors with an air-filled cavity behind the elastic body. By changing a pressure of the cavity, we will be able to control easily a deepness of contact as well as a touching force.

References

[1] H. R. Nicholls and M. H. Lee, "A Survey of Robot Tactile Sensing Technology", Int. J. Robotics Res., Vol.8, No.3, pp.3-30, 1989.

[2] L. D. Harmon, "Automated Tactile Sensing", Int. J. Robotics Res., Vol. 1, No. 2, pp.3-32, 1982.

[3] L. D. Harmon, "Tactile Sensing for Robot, Recent Advances in Robotics", G.Beni and S. Hackwood eds., John Wiley & Sons, pp.389-424, 1985.

[4] M.Ishikawa, "Sensor Fusion -Mechanism for Integration of Sensory Information-", Proc. 9th Sensor Symposium, Tokyo, pp.153-158, 1990.

[5] R. F. Schmidt ed., "Fundamentals of Sensory Physiology", Chap.2, Springer-Verlag, 1986.

[6] R.D.Howe, "A Tactile Stress Rate Sensor for Perception of Fine Surface Features", IRANSDUCERS '91: Proceedings of the 6th International Conference on Solid State Sensors and Actuators, IEEE Electron Devices Society, San Francisco, June, pp.864-867, 1991.

[7] R.S.Fearing, "Tactile Sensing Mechanisms", Int. J. Robotics Res., Vol. 9, No. 3, pp.3-23, 1990.

[8] D.DeRossi et al., "Fine-form Tactile Discrimination through Inversion of Data from a Skin-like Sensor", Proceedings of the 1991 IEEE International Conference on Robotics and Automation, Sacramento, CA, April, pp.398-404, 1991.

[9] H.Shinoda and S.Ando, "A Tactile Sensing Algorithm based on Elastic Transfer Function of Surface Deformation", Proc.IEEE ICASSP'92, Vol.3, pp.589-592, San Francisco, 1992.

[10] S. P. Timoshenko and J. N. Goodier, "Theory of Elasticity", Chap. 12, McGraw-Hill, 1970.

[11] P. Dario and G. Buttazzo, "An Anthropomorphic Robot Finger for Investigating Artificial Tactile Perception", Int. J. Robotics Res., Vol.6, No.3, pp.25-48, 1987.

[12] D. De Rossi, et al., "Biomimetic Tactile Sensor with Stress-Component Discrimination Capability", J. Molecular Electronics, Vol.3, pp.173-181, 1987.

[13] R. D. Howe, "A Force Reflecting Teleoperated Hand System for the Study of Tactile Sensing in Precision Manipulation", Proc. 1992 IEEE Int. Conf. Robotics and Automation, pp.1321-1326, Nice,France,May 1992.